Sensors and Materials, Vol. 35, No. 4 (2023) 1413–1423
MYU Tokyo

S & M 3256

Adsorption Properties of Pt/N-doped Graphene for SF_6 Decomposition Species

Dongyue Wu,[1*] Linxi Zhou,[2**] Chao Chen,[1] and Xuehui Liang[1]

[1]Tianjin Key Laboratory for Control Theory and Applications in Complicated Systems, Tianjin University of Technology, Tianjin 300384, China
[2]School of Materials Science and Engineering, Hebei University of Technology, Tianjin 300130, China

(Received August 9, 2022; accepted January 16, 2023)

Keywords: graphene-based carrier, SO_2, density functional theory (DFT), SF_6 decomposition products

In this paper, using density functional theory, we studied the adsorption properties of four different structures of Pt- and N-doped graphene (Pt/*x*N-GN, x = 0,1,2,3) for SO_2, the main decomposition product of SF_6. In the Pt/*x*N-GN structure, with increasing N atom content, the adsorption distance of SO_2 decreases and the adsorption energy increases. The total density of states and the partial density of states of the system before and after gas adsorption were compared and analyzed to explore the mechanism of the interaction between SO_2 and the Pt/*x*N-doped graphene structure. Pt/3N-GN adsorbs SO_2 gas molecules, and orbital hybridization occurs, which is chemical adsorption. Pt/3N-GN has good adsorption performance for SO_2 gas molecules, and the adsorption energy is −2.548 eV. The gas sensor based on Pt/*x*N-doped graphene studied in this paper has good application prospects in the field of gas-insulated switchgear discharge decomposition component detection and fault diagnosis.

1. Introduction

SF_6 is a strongly electronegative gas with excellent insulation performance, arc extinguishing ability, and good chemical stability; thus, it is widely used in gas-insulated switchgear (GIS) in power systems.(1) Partial discharge usually occurs when there are latent insulation defects inside power equipment. Under the action of partial discharge energy, the insulating gas SF_6 inside GIS decomposes to produce several low-fluorine sulfides (SF*x*, x = 1–5) and F atoms.(2) Moisture and oxygen in the atmosphere can react with SF*x* to form a variety of gases, one of which is SO_2.(3) These compounds can damage insulating materials and thus cause accidents.(4) Therefore, the online monitoring of SF_6 decomposition products to evaluate the operation status of electrical equipment has become the focus of research in this field.(5,6) An urgent task is to find a new gas sensor that can be used for online monitoring of the decomposition components of SO_2.

Graphene, a typical 2D carbon nanomaterial composed of carbon atoms hybridized with sp^2 orbitals, was discovered by researchers in 2004. Graphene has attracted much attention because of its low electronic noise, high surface-area-to-volume ratio, and excellent optical and charge

*Corresponding author: e-mail: tsam0925@163.com
**Corresponding author: e-mail: zhoulinxi@hebut.edu.cn
https://doi.org/10.18494/SAM4079

ISSN 0914-4935

transfer properties.[7,8] It has been found that the adsorption of gas molecules changes the conductivity of graphene molecules, making it possible for graphene to be used in gas detection.[9,10] This is because when graphene interacts with gas molecules, the charge transfer changes the conductivity of graphene, and this change can be used as a signal to detect gas molecules.[11] However, many studies have shown that intrinsic graphene is almost insensitive to most gas molecules owing to its weak interaction with them. To overcome this shortcoming, graphene has been modified by doping with other atoms[12–15] to improve its gas sensing properties for specific molecules. Girit *et al.* embedded transition metal atoms into a graphene substrate (TM/GN), which improved the active range of the graphene adsorption reaction.[16] Pt nanoparticles have excellent sensing ability, catalytic activity, and high specific surface area, and have been widely used in catalysis, sensors, fuel cells, optical devices, and other fields. Liu *et al.* studied the capacity of a graphene group embedded with Pt to adsorb CO.[17] Liu *et al.* studied the capacity of a Pt-embedded single vacancy and different pyridinic N-doped graphene carriers to adsorb O_2.[18] Many studies have shown that Pt-doped graphene has good gas sensing properties.[17–19] Doping nonmetallic N atoms into graphene monolayer materials can increase their chemical activity and carrier mobility while retaining structural stability similar to that of graphene. These outstanding characteristics make Pt- and N-doped graphene the most promising graphene functional materials.[20,21] In this study, by first-principles calculation based on density functional theory (DFT), we analyze and study the gas sensing characteristics of Pt/N-codoped graphene materials for SO_2, the main decomposition component of SF_6, so as to provide a theoretical basis for the development of new gas sensors for SF_6.

2. Calculation Method

All calculations were conducted in the Dmol^3 package.[22] In this study, exchange-related generalized gradient approximation (GGA) was used, and the Perdew–Burke–Ernzerhof (PBE) functional was used to consider the exchange crosslinking between electrons.[22] The combined use of the PBE functional and the Grimme dispersion correction is considered to be the most suitable theoretical method for studying the interaction between molecules and graphene.[23] Using the Grimme dispersion correction (the C6 and R0 parameters of Pt atoms used for the Grimme dispersion correction were obtained by the DFT-D3 query then input into Dmol^3), DFT semi-core pseudopotential (DSSP) were selected to replace the mononuclear electron effective potential.[24] A double numerical basis with polarization functions (DNP) was selected as the atomic orbital basis.

A 5 × 5 × 1 single-layer graphene supercell model, which was composed of 50 carbon atoms, was constructed. Its boundary conditions were periodic in the X and Y directions to simulate infinite graphene sheets. A vacuum region of 20 Å (1 Å = 10^{-10} m) was set to prevent the interaction between adjacent units. The C–C bond length of graphene after structural optimization was 2.47 Å, which is close to the theoretical and experimental values, indicating the correctness of the model.

The energy convergence accuracy, maximum stress, and maximum displacement were respectively set to 1×10^{-5} Ha (1 Ha = 27.212 eV), 2×10^{-3} Ha/Å, and 5×10^{-3} Å.[25] During the

structural optimization and electronic property calculations, the corresponding k-points were set to 5 × 5 × 1 and 9 × 9 × 1, respectively. The convergence accuracy of the self-consistent field was set to 1 × 10^{-6} Ha.[26] The direct inversion in the iterative subspace (DIIS) was set to 6, which improves the convergence speed of the self-consistent field charge density, thereby improving the efficiency.[27]

The binding energy E_b formed by the interaction between the Pt dopant and the matrix is obtained as

$$E_b = E_{Pt/xN\text{-}GN} - E_{sub} - E_{Pt}, \tag{1}$$

where $E_{Pt/xN\text{-}GN}$ is the total energy of Pt/*x*N-GN, E_{sub} is the energy of the *x*N-doped graphene with one C atom defect, and E_{Pt} is the energy of a Pt atom.

The adsorption energy E_{ads} of gas molecules on the surface of doped graphene is

$$E_{ads} = E_{Pt/xN\text{-}GN\text{-}gas} - E_{Pt/xN\text{-}GN} - E_{gas}, \tag{2}$$

where $E_{Pt/xN\text{-}GN\text{-}\mathrm{gas}}$ is the total energy of the Pt/*x*N-GN-adsorbed SO_2 gas and E_{gas} is the energy of SO_2. If the calculated adsorption energy is negative, then the adsorption is exothermic, can occur spontaneously, and is stable. The greater the absolute value of the adsorption energy, the greater the change in total energy in the adsorption process and the stronger the interaction between the sensing material and the adsorbed gas.

The Hirshfeld charge analysis method[28] is used to calculate and analyze the charge transfer (Q_t) between gas molecules and the Pt-doped graphene structure:

$$Q_t = Q_a - Q_b, \tag{3}$$

where Q_a and Q_b represent the total charges of gas molecules after and before adsorption, respectively.

3. Results and Analysis

3.1 Adsorption of SO_2 by intrinsic graphene

The optimized SO_2 molecular model is shown in Fig. 1. The S–O bond length is 1.465 Å, and the O–S–O bond angle is 119.695°. The calculation results are close to the theoretical value for SO_2 (the S–O bond length is 1.43 Å and the bond angle is 119.536°), which proves the reliability of this calculation. To compare the difference in adsorption capacity before and after Pt/N doping, the adsorption of SO_2 on the surface of intrinsic graphene was studied. Many researchers have studied the adsorption of SO_2 by intrinsic graphene. Drawing on other research results,[3] we only simulate the key adsorption structure, which is shown in Fig. 2.

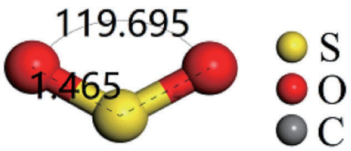

Fig. 1. (Color online) Optimized SO_2 molecular model.

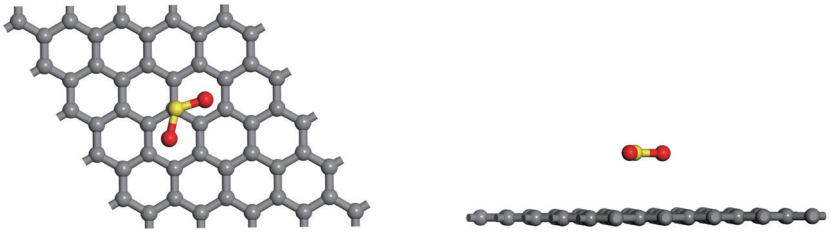

(a) (b)

Fig. 2. (Color online) Adsorption structure of SO_2 on intrinsic graphene surface. (a) Top and (b) side views.

Table 1
Adsorption parameters of SO_2 on intrinsic graphene.

Sensing material	Adsorption energy E_{ads} (eV)	Transfer charge Q_t (e)	Adsorption distance d (Å)
GN	−0.442	−0.067	3.165

The adsorption parameters of SO_2 on the surface of intrinsic graphene are shown in Table 1. The adsorption distance d is 3.165 Å, the transfer charge Q_t is −0.067 e, and the adsorption energy E_{ads} is −0.442 eV. After adsorption, the bond length and angle of SO_2 change only slightly, indicating that the adsorption is mainly physical adsorption and is not strong.

3.2 Pt/N doping on graphene

To study the adsorption performance of Pt/N-codoped-graphene-based sensing materials for SO_2, a Pt/GN graphene system loaded with Pt atoms is built. A single Pt atom replaces one carbon atom in graphene and is connected with three carbon atoms. The Pt atom is embedded into the graphene plane and does not adsorb on a carbon atom. The Pt/GN structure after structural optimization is shown in Fig. 3(a), with the top view shown on the left and the side view shown on the right. The three carbon atoms connected with Pt can be replaced by N atoms to form three sensing material systems, namely, Pt/1N-GN, Pt/2N-GN, and Pt/3N-GN, whose optimized structures are shown in Figs. 3(b)–3(d), respectively.

The calculated structural parameters such as the distance h from the Pt atom to the plane of graphene, the bond lengths between the Pt atom and the connected C and N atoms, $d_{Pt–C}$ and $d_{Pt–N}$, respectively, and the binding energy E_b between Pt and the substrate are shown in Table 2.

The calculated results in this paper are basically consistent with those reported in the literature.[29] The calculated structural parameters in Table 2 are also basically consistent with

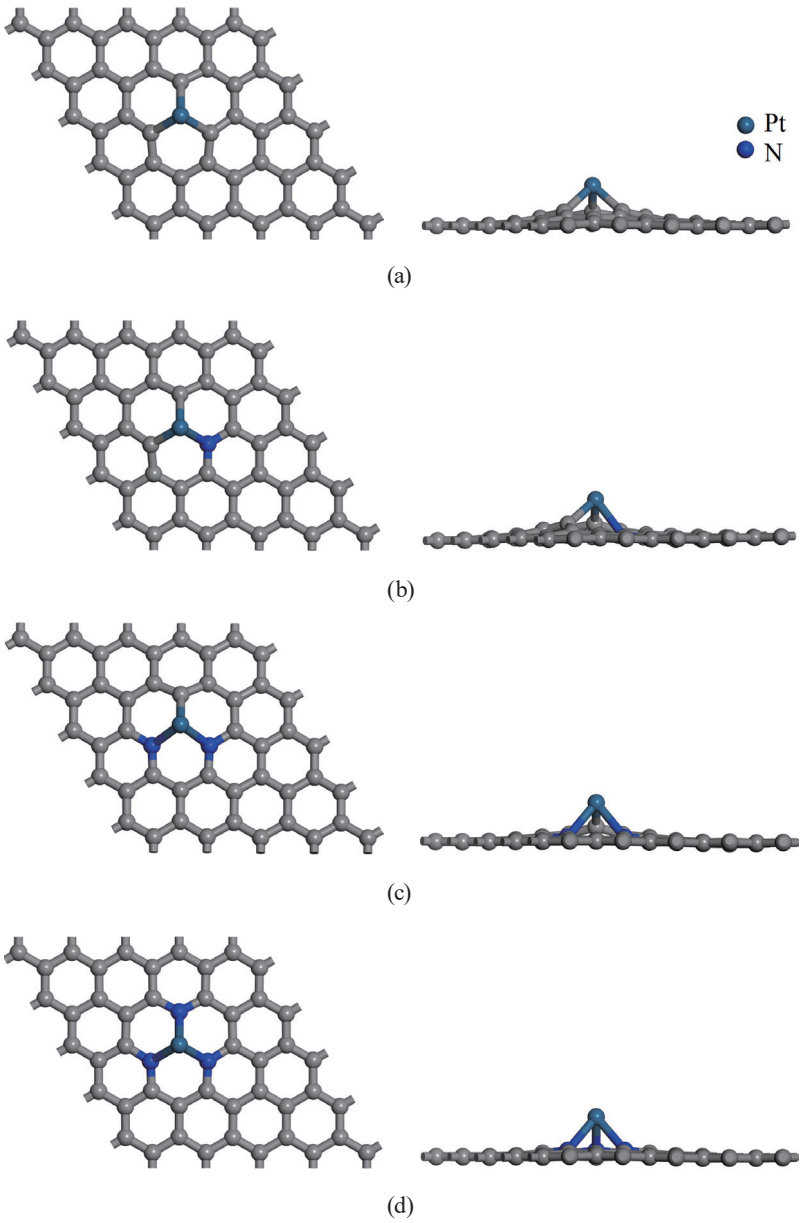

Fig. 3. (Color online) Top and side views of structures of Pt/*x*N-GN. (a) Pt/GN, (b) Pt/1N-GN, (c) Pt/2N-GN, and (d) Pt/3N-GN.

those in the literature, indicating that they are reasonable and reliable. A Pt atom has a larger volume than a C atom. When a Pt atom is embedded into graphene, owing to the steric hindrance effect and tension, the Pt atom remains a certain distance from the plane of graphene. For Pt/GN, Pt/1N-GN, Pt/2N-GN, and Pt/3N-GN, the distances from the Pt atom to the C atom plane are 1.56, 1.71, 1.75, and 1.78 Å, respectively. This shows that with increasing concentration of doped N atoms, the distance between the Pt atom and the C atom plane also increases. The binding energy of Pt/*x*N-GN decreases with increasing nitrogen doping rates. When there are three N atoms, the binding energy is −3.15 eV and the structure has high stability.

Table 2
Structural parameters of Pt- and N-doped graphene.

Sensing material	h (Å)	d_{Pt-C} (Å)	d_{Pt-N} (Å)	E_b (eV)
Pt/GN	1.56	2.01	—	−7.75
	1.58[29]	1.94[29]	—	−7.37[29]
Pt/1N-GN	1.71	1.94	2.35	−5.50
	1.66[29]	1.94[29]	2.27[29]	−5.15[29]
Pt/2N-GN	1.75	1.92	2.20	−4.77
	1.68[29]	1.92[29]	2.18[29]	−4.58[29]
Pt/3N-GN	1.78	—	2.16	−3.15
	1.73[29]	—	2.16[29]	−2.90[29]

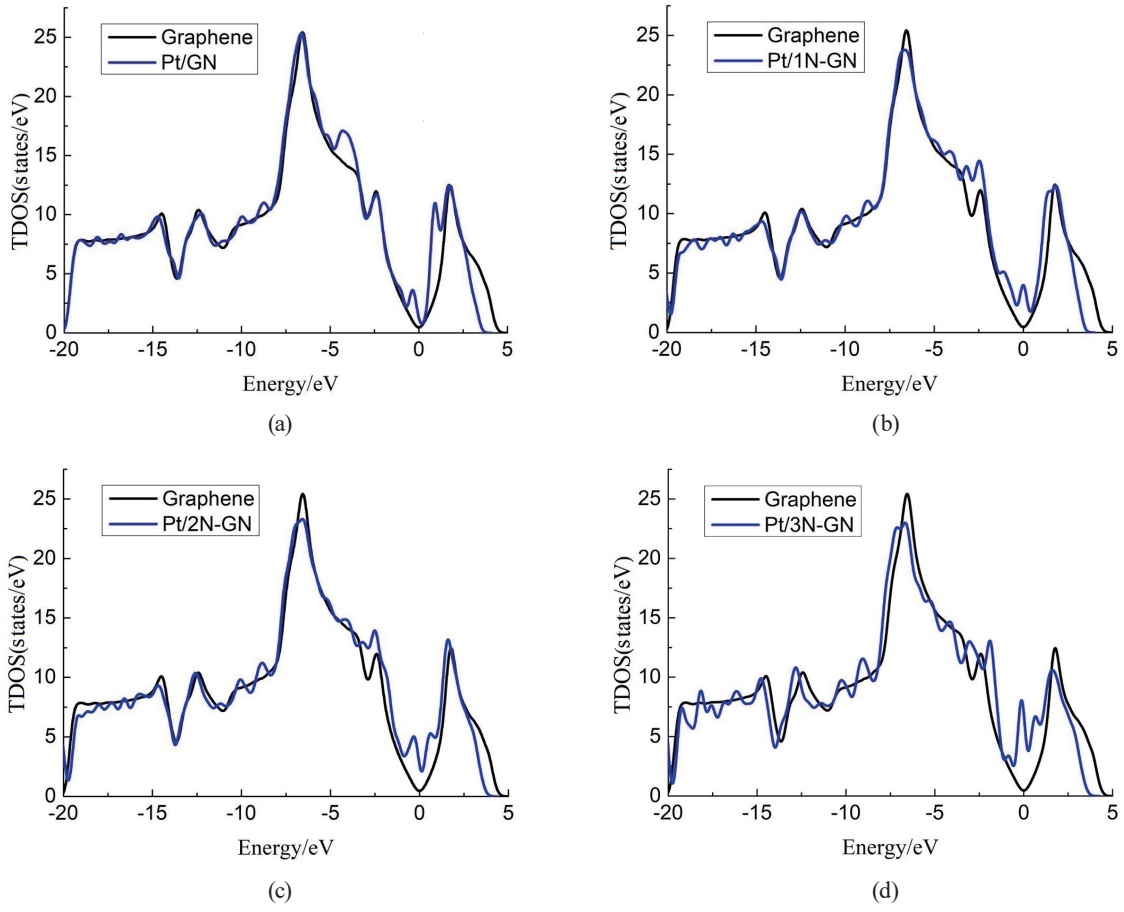

Fig. 4. (Color online) TDOS values of graphene before and after doping Pt/N. (a) Pt/GN TDOS, (b) Pt/1N-GN TDOS, (c) Pt/2N-GN TDOS, and (d) Pt/3N-GN TDOS.

The total density of states (TDOS) values of the four Pt/*x*N-GN systems and intrinsic graphene are shown in Fig. 4. It is found that after doping Pt/N, the electron distribution near the Fermi level of the TDOS is significantly higher than that of the intrinsic graphene, and the greater the number of N atoms, the more obvious the change in electron distribution near the Fermi level. This shows that the doping of Pt and N atoms enhances the conductivity of the graphene structure, which may improve its sensitivity to SO_2.

3.3 SO_2 adsorption on Pt/*x*N-GN

To obtain the optimal adsorption configuration, we consider the approach of the SO_2 gas molecules to the Pt/*x*N-GN system at different angles and positions. After full optimization, the most stable structures for gas adsorption with the lowest energy are shown in Fig. 5. The relevant structural parameters such as bond angle, bond length, charge transfer, and adsorption energy are listed in Table 3.

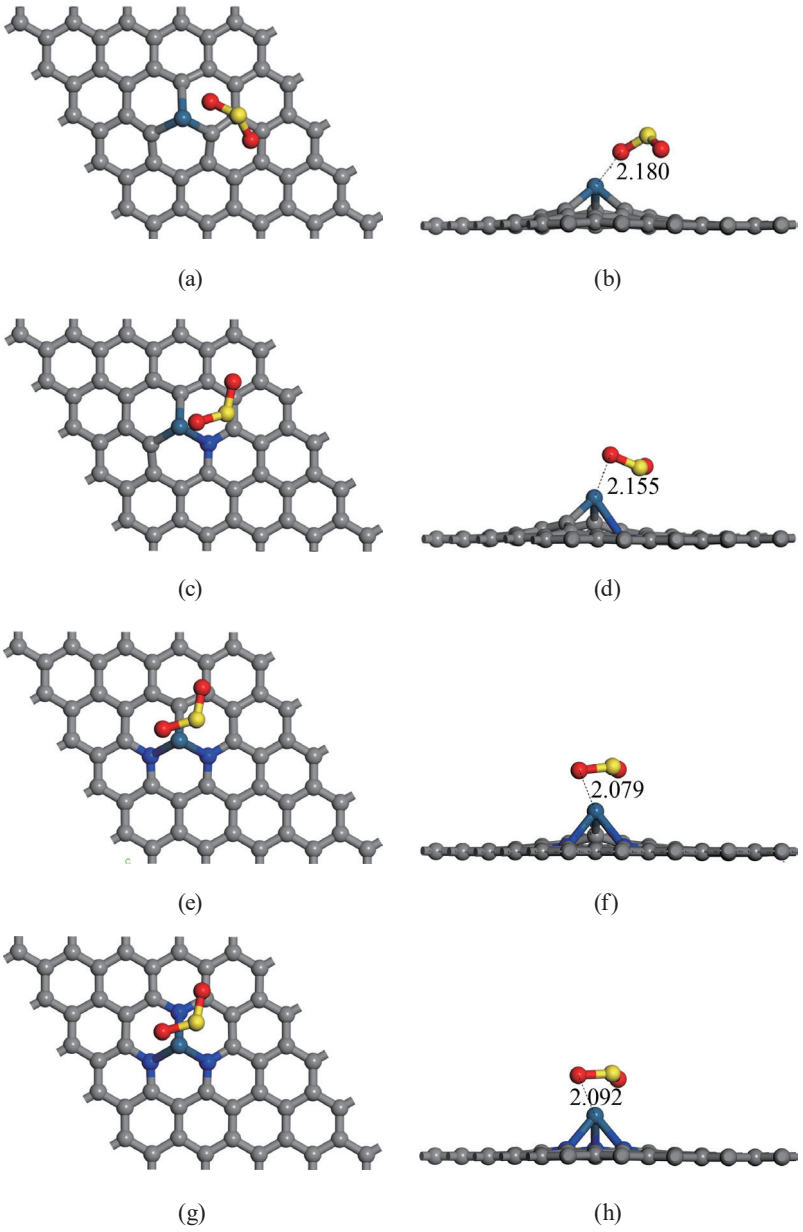

Fig. 5. (Color online) Adsorption structures of SO_2 on Pt/*x*N-GN. (a) Pt/GN top view, (b) Pt/GN side view, (c) Pt/1N-GN top view, (d) Pt/1N-GN side view, (e) Pt/2N-GN top view, (f) Pt/2N-GN side view, (g) Pt/3N-GN top view, and (h) Pt/3N-GN side view.

Table 3
Adsorption parameters of SO_2 on Pt/*x*N-GN.

Sensing material	Bond angle of SO_2	d_{S-O1} (Å)	d_{S-O2} (Å)	d_{O-Pt} (Å)	d_{S-Pt} (Å)	Q_t (e)	E_{ads} (eV)
Pt/GN	114.689	1.549	1.488	2.180	3.382	−0.195	−1.020
Pt/1N-GN	114.985	1.561	1.478	2.155	2.639	−0.175	−1.061
Pt/2N-GN	114.910	1.609	1.480	2.079	2.392	−0.241	−2.087
Pt/3N-GN	115.034	1.610	1.488	2.092	2.316	−0.352	−2.548

It can be seen from Table 3 that in the Pt/GN structure, the adsorption of SO_2 is mainly between Pt and O. One O atom in SO_2 is adsorbed by a Pt atom with a bond length of 2.180 Å (d_{O-Pt}), which means that the adsorption is chemical adsorption. Owing to the strong interaction between O and Pt bonds, the bond length (d_{S-O1}) of S–O with the O atom adsorbed by Pt increases to 1.549 Å. The bond length (d_{S-O2}) of the other O atom not adsorbed by Pt changes negligibly and is 1.488 Å. The charge transfer Q_t of this system is 0.195 e, indicating that there is charge transfer from the Pt/GN substrate to SO_2. The adsorption energy of SO_2 for this system is −1.020 eV, which is much larger than that of the intrinsic graphene.

In the Pt/1N-GN system, the O–Pt bond length between the O atom of SO_2 and the Pt atom of the system is 2.155 Å, which means that the adsorption is chemical adsorption. The bond length of S–O formed by the O atom adsorbed by the Pt atom in the SO_2 molecule is 1.561 Å. The adsorption energy of SO_2 molecules in this system is −1.061 eV. Compared with the Pt/GN system, the overall adsorption energy shows little change, and this system does not show a significant improvement compared with the Pt/GN system.

In the Pt/2N-GN system, the O–Pt bond length between the O atom of SO_2 and the Pt atom of the system is 2.079 Å, which means that the adsorption is chemical adsorption. The bond length of S–O formed by the O atom adsorbed by the Pt atom in the SO_2 molecule is 1.609 Å. The adsorption energy of SO_2 molecules increases to −2.087 eV. Compared with the above two systems, the adsorption energy of SO_2 by the Pt/2N-GN system is significantly larger and the adsorption capacity is greater.

In the Pt/3N-GN system, the O–Pt bond length is 2.092 Å, which means that the adsorption is chemical adsorption. The bond length of S–O formed by the O atom adsorbed by the Pt atom in the SO_2 molecule is 1.610 Å. The adsorption energy of SO_2 molecules increases to −2.548 eV, and the adsorption effect is the strongest among the systems. These calculation results show that with increasing number of doped N atoms, the adsorption of SO_2 by the Pt/*x*N-GN system gradually increases.

To further study the adsorption mechanism of the Pt/2N-GN and Pt/3N-GN systems with the greatest adsorption capacity for SO_2, their adsorption mechanism and the TDOS and partial density of states (PDOS) of the main interacting atoms are analyzed in detail, and the results are shown in Figs. 6 and 7.

It can be seen from Fig. 6 that the TDOS of the Pt/2N-GN structure markedly changes at −20.5, −11.4, −6.2, and −3 eV. Because the outermost electrons of the atoms contribute the most to the adsorption process, the PDOS diagrams of S–3p, Pt–5d, and O–2p are compared and analyzed. The PDOS shows peaks at −20.5, −11.4, −7, −5.1, −2.7, and −2 eV and other energy

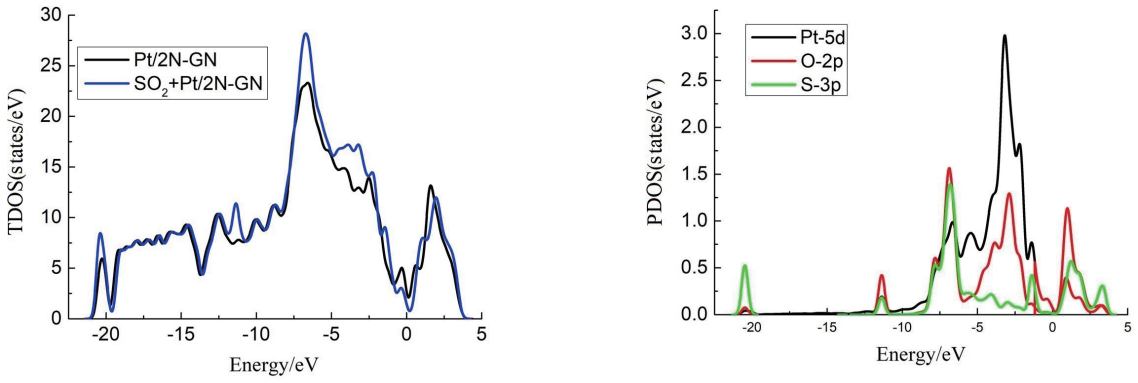

(a) (b)

Fig. 6. (Color online) TDOS before and after SO_2 adsorption and PDOS of the main interacting atoms in the Pt/2N-GN system. (a) TDOS of Pt/2N-GN system and (b) PDOS of Pt/2N-GN system

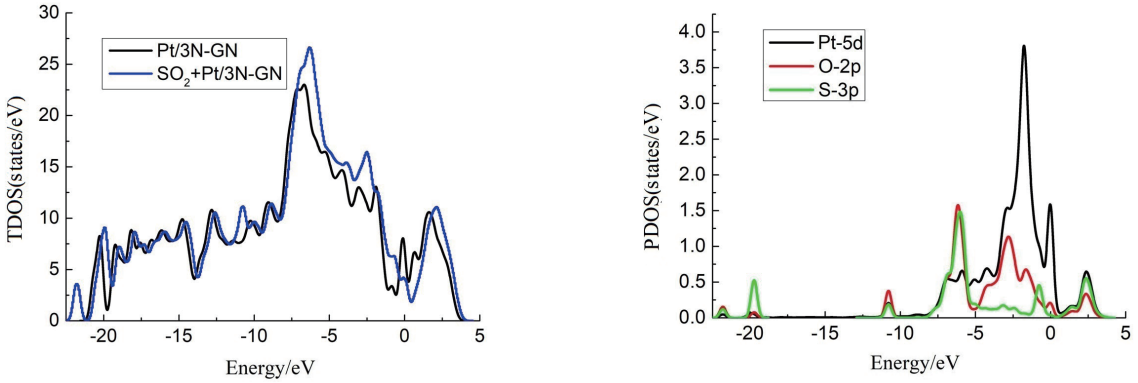

(a) (b)

Fig. 7. (Color online) TDOS before and after SO_2 adsorption and PDOS of the main interacting atoms in the Pt/3N-GN system. (a) TDOS of Pt/3N-GN system and (b) PDOS of Pt/3N-GN system.

levels at the same time, indicating that orbital hybridization exists in the adsorption structure, which means that there is strong chemical adsorption between SO_2 gas and Pt/2N-GN.

It can be seen from Fig. 7 that the TDOS of the Pt/3N-GN structure markedly changes at −22, −20.5, −11.4, −6.8, and −2.7 eV. The PDOS shows peaks at −22, −20, −11, −7, −2.7, −2, and 0 eV and other energy levels at the same time, indicating that orbital hybridization exists in the adsorption structure, which means that the adsorption between SO_2 gas and Pt/3N-GN is also chemisorption. Compared with the Pt/2N-GN structure, the center of the d-band of the Pt atom in the Pt/3N-GN structure shifts to the right to a large extent and is closer to the Fermi level, indicating that the orbital hybridization of this structure is stronger and that the adsorption of SO_2 is greater.

4. Conclusions

We performed a first-principles calculation to theoretically study the adsorption characteristics of graphene sensor materials for SO_2 gas, build an adsorption model for SO_2 by Pt doping on graphene substrates with different N contents, and study the adsorption configuration, relevant structural parameters, adsorption energy, and electronic properties of SO_2 on Pt/*x*N-GN. The results show that different graphene substrates have markedly different adsorption effects on SO_2. The adsorption energies of Pt/GN, Pt/1N-GN, and Pt/2N-GN for SO_2 gas are −1.020, −1.061, and −2.087 eV, respectively. The adsorption energy of Pt/3N-GN for SO_2 gas is the highest (−2.548 eV), indicating that the doping of N improves the adsorption capacity. The interaction between SO_2 and Pt/3N-GN is strong, and the adsorption between SO_2 and Pt/3N-GN is chemical adsorption. The results of this paper provide a new concept for developing a gas sensor based on Pt/N-codoped graphene to realize the online fault detection of SF_6 insulation equipment.

References

1 H. Cui, C. Yan, and P. Jia: Appl. Surf. Sci. **512** (2020) 145759. https://doi.org/10.1016/j.apsusc.2020.145759
2 X. Zhang, Y. Lei, Y. Gui, and H. Weihua: Appl. Surf. Sci. **367** (2016) 259. https://doi.org/10.1016/j.apsusc.2016.01.168
3 X. Gao, Q. Zhou, J. Wang, L. Xu, and W. Zeng: Appl. Surf. Sci. **517** (2020) 146180. https://doi.org/10.1016/j.apsusc.2020.146180
4 D. Wang, X. Wang, A. Yang, J. Chu, P. Lv, Y. Liu, and M. Rong: IEEE Electron Device Lett. **39** (2017) 292. https://doi.org/10.1109/LED.2017.2786322
5 H. Cui, X. Zhang, J. Zhang, and Y. Zhang: High Voltage **4** (2019) 242. https://doi.org/10.1049/hve.2019.0130
6 J. Tang, F. Liu, Q. Meng, X. Zhang, and J. Tao: IEEE Electron Device Lett. **19** (2012) 37. https://doi.org/10.1109/TDEI.2012.6148500
7 H. Mao, S. Laurent, W. Chen, O. Akhavan, M. Imani, A. Ashkarran, and M. Mahmoudi: Chem. Rev. **113** (2013) 3407. https://doi.org/10.1021/cr300335p
8 Q. Zhou, W. Ju, X. Su, Y. Yong, and X. Li: J. Phys. Chem. Solids. **109** (2017) 40. https://doi.org/10.1016/j.jpcs.2017.05.007
9 P. Majzlíkov, J. Sedláček, J. Prášek, J. Prášek, J. Pekárek, V. Svatoš, A. Bannov, O, Synek, M. Eliáš, L. Zajíčková, and J. Hubálek: Sensors **15** (2015) 2644. https://doi.org/10.3390/s150202644
10 Y. Tang, W. Chen, C. Li, L. Pan, X. Dai, and D. Ma: Appl. Surf. Sci. **342** (2015): 191. https://doi.org/10.1016/j.apsusc.2015.03.056
11 R. Pearce, T. Iakimov, M. Andersson, L. Hultman, A. Spetz, and R. Yakimova: Sens. Actuators, B **155** (2011) 451. https://doi.org/10.1016/j.snb.2010.12.046
12 Y. Li, K. Li, X. Sun, X. Song, H. Sun, and P. Ning: J. Mol. Model. **25** (2019) 358. https://doi.org/10.1007/s00894-019-4227-9
13 L. Velázquez-López, S. Pacheco-Ortin, R. Mejía-Olvera, and E. Agacino-Valdés: J. Mol. Model. **25** (2019) 91. https://doi.org/10.1007/s00894-019-3973-z
14 Y. Zhang, H. Zhang, T. Chen, Z. Zhang and L. An: Nano **16** (2021) 2150105. https://doi.org/10.1142/S1793292021501058
15 Y. Tang, Z. Liu, X. Dai, Z. Yang, W. Chen, D. Ma, and Z. Lu: Appl. Surf. Sci. **308** (2014) 402. https://doi.org/10.1016/j.apsusc.2014.04.189
16 O. Girit, J. Meyer, R. Erni, M. Rossell, C. Kisielowski, L. Yang, C. Park, M. Crommie, M. Cohen, and S. Louie: Science **323** (2009) 1705. https://doi.org/10.1126/science.1166999
17 X. Liu, Y. Sui, T. Duan, C. Meng, and Y. Han: Phys. Chem. Chem. Phys. **16** (2014) 23584. https://doi.org/10.1039/c4cp02106a
18 S. Liu and S. Huang: Carbon **115** (2017) 11. https://doi.org/10.1016/j.carbon.2016.12.094
19 E. Salih and A. Ayesh: Mate. Chem. Phys. **267** (2021) 124695. https://doi.org/10.1016/j.matchemphys.2021.124695
20 M. Zhu, C. Zhai, M. Sun, Y. Hu, B. Yan, and Y. Du: Appl. Catal. B **203** (2017) 108. https://doi.org/10.1016/j.apcatb.2016.10.012

21 Z. Yue, A. Liu, C. Zhang, J. Huanga, M. Zhu, Y. Du, and P. Yang: Appl. Catal. B **201** (2017) 202. https://doi.org/10.1016/j.apcatb.2016.08.028
22 H. Cui, K. Zheng, L. Tao, J. Yu, and X. Chen: IEEE Electron Device Lett. **40** (2019) 1522. https://doi.org/10.1109/LED.2019.2926886
23 V. Basiuk and L. Henaoholguín: J. Comput. Theor. Nanosci. **11** (2014) 1609. https://doi.org/10.1166/jctn.2014.3539
24 H. Cui, D. Chen, Y. Zhang, and X. Zhang: Sustainable Mater. Technol. **20** (2019) 94. https://doi.org/10.1016/j.susmat.2019.e00094
25 X. He, Y. Gui, J. Xie, X. Liu, Q. Wang, and C. Tang: Appl. Surf. Sci. **500** (2020) 144030. https://doi.org/10.1016/j.apsusc.2019.144030
26 H. Cui, G. Zhang, X. Zhang, and J. Tang: Nanoscale Adv. **2** (2019) 772. https://doi.org/10.1039/C8NA00233A
27 Y. Gui, W. Li, X. He, Z. Ding, C. Tang, and L. Xu: Appl. Surf. Sci. **507** (2020) 145163. https://doi.org/10.1016/j.apsusc.2019.145163
28 C. Liu, C. Liu, and X. Yan: Phys. Lett. A. **381** (2017) 1092. https://doi.org/10.1016/j.physleta.2017.01.048
29 Z. Gao, X. Li, A. Li, C. Ma, X. Liu, J. Yang, and W. Yang: Appl. Organomet. Chem. **34** (2019) 1. https://doi.org/10.1002/aoc.5079

About the Authors

Dongyue Wu received his B.S. degree from Hebei University of Technology, China, in 2005 and his M.S. and Ph.D. degrees from Tianjin University, China, in 2008 and 2012, respectively. Since 2012, he has been a lecturer at Tianjin University of Technology, China. His research interests are in multisensor fusion, detection signal analysis, and the fault diagnosis of processing and insulation equipment. (tsam0925@163.com)

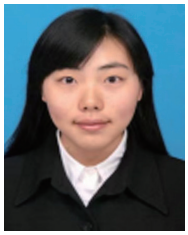

Linxi Zhou received her B.S. degree from Hebei Normal University, China, in 2005 and her M.S. degree from Nankai University, China, in 2009. Since 2011, she has been a researcher at Hebei University of Technology, China. Her research interests are in the synthesis, preparation, and performance research of materials. (zhoulinxi@hebut.edu.cn)

Chao Chen received his B.S. degree in automation and his M.S. degree in pattern recognition and intelligent systems from Northeastern University, Shenyang, China, in 2005 and 2008, respectively. In 2014, he received his Ph.D. degree from Tokyo Institute of Technology, Japan. Currently, he is a professor in School of Electrical Engineering, Tianjin University of Technology. He mainly works on invasive and noninvasive brain–computer interfaces, pattern recognition, and intelligent algorithms.
(cccovb@hotmail.com)

Xuehui Liang received her B.S. degree from Wuhan University of Water Resources and Electric Power (now Wuhan University), China, in 1993 and her M.S. degree from Nagoya University, Japan, in 2006. Since 2010, she has been an assistant professor at Tianjin University of Technology, China. Her research interests are in the development of monitoring systems.
(1733171283@qq.com)